Journal of Sound and Vibration (2002) **255**(4), 663–684
doi:10.1006/jsvi.2001.4183, available online at http://www.idealibrary.com on IDEAL®

ON THE RELATION BETWEEN COMPLEX MODES AND WAVE PROPAGATION PHENOMENA

K. M. Ahmida and J. R. F. Arruda

Departamento de Mecânica Computacional, FEM, Universidade Estadual de Campinas, C. P. 6122, *Campinas, SP, Brazil. E-mails*: *khaled@fem.unicamp.br*; *arruda@fem.unicamp.br*

(*Received* 29 *May* 2001, *and in final form* 27 *November* 2001)

This paper discusses the well-known, but often misunderstood, concept of complex modes of dynamic structures. It shows how complex modes can be interpreted in terms of wave propagation phenomena caused by either localized damping or propagation to the surrounding media. Numerical simulation results are presented for different kinds of structures exhibiting modal and wave propagation characteristics: straight beams, an L-shaped beam, and a three-dimensional frame structure. The input/output transfer relations of these structures are obtained using a spectral formulation known as the spectral element method (SEM). With this method, it is straightforward to use infinite elements, usually known as throw-off elements, to represent the propagation to infinity, which is a possible cause of modal complexity. With the SEM model, the exact dynamic behavior of structures can be investigated. The mode complexity of these structures is investigated. It is shown that mode complexity characterizes a behavior that is half-way between purely modal and purely propagative. A coefficient for quantifying mode complexity is introduced. The mode complexity coefficient consists of the correlation coefficient between the real and imaginary parts of the eigenvector, or of the operational deflection shape (ODS). It is shown that, far from discontinuities, this coefficient is zero in the case of pure wave propagation in which case the plot of the ODS in the complex plane is a perfect circle. In the other extreme situation, a finite structure without damping (or with proportional damping), where the mode shape (or the ODS) is a straight line on the complex plane, has a unitary complexity coefficient. For simple beam structures, it is shown that the mode complexity factor can also be calculated by curve-fitting the mode to an ellipse and computing the ratio of its radii.

1. INTRODUCTION

In the past few decades, the structural dynamics community has been most oblivious to the wave propagation approach, which nearly disappeared from undergraduate mechanical vibrations and structural dynamics textbooks, outmatched by the modal approach. With the growing interest for higher frequency dynamics and vibroacoustics in recent years, there is a comeback of the wave propagation approach to vibration analysis. At higher frequencies, boundary conditions cannot be modelled ideally as simply supported or clamped. The interaction with the surrounding media, solid or fluid, must be taken into account. Waves propagating to neighboring structures represent energy dissipation, and the phenomenon is usually taken into account in modal models via modal damping coefficients. Damping caused by wave propagation should be taken into consideration, as it can be an important source of modal complexity. Another source is non-proportional internal damping, which represents localized energy dissipation within the structure.

0022-460X/02/$35.00

Modes are due to the superposition of waves reflecting at the boundaries or at material and geometric discontinuities of a finite structure. Real modes result when damping is well distributed within the structure. For a discrete system, this means that the damping matrix is a linear combination of the stiffness and mass matrices or, more generally, that the three matrices satisfy a well-known algebraic relation [1].

For a linear discrete structure represented by these three matrices, complex modes can be computed by transforming the second order ordinary algebraic system of equilibrium equations into a double-sized first order algebraic system of equations. Depending upon the choice of the state-space variables, one non-symmetric or two-symmetric system matrices are obtained, and an eigenvalue problem may be solved. The eigenvalues and eigenvectors exhibit the orthogonality property and can be treated as mode shapes. They are, in general, complex. The question that arises is how to physically interpret those complex mode shapes. Infinite structures, on the other hand, do not exhibit real-mode shapes, but due to discontinuities may exhibit local-mode shapes. Infinite structures must be analyzed using wave propagation or spectral formulations.

Both types of linear structures—finite and infinite—when excited by a sinusoidal force with a certain frequency (many sinusoidal forces at different locations and frequencies can be treated by superposition), present a stationary vibration pattern at that same frequency. This is usually known as the operational deflection shape (ODS). ODS can be defined as the spatial distribution of magnitude and phase of the structure deflection, at a given frequency. The ODS can be measured directly by simple means and it can provide very useful information to understand and evaluate the dynamic behavior of a structure. Operational deflection shapes are, in general, complex quantities, even in the case of proportionally damped structures.

Modal complexity is usually attributed to non-proportional damping. However, it can also arise from gyroscopic effects, aerodynamic effects, non-linear structural behavior, experimental noise effects, aliasing, leakage, mass loading, high modal density, and identification errors [2, 3]. Many other authors have reviewed and investigated complex mode shapes [4–6]. Oliveto *et al.* [7] presented a numerical methodology, which is based on a modal superposition, to evaluate complex modes of a simply supported beam with a rotational viscous damping. A relation between the real and imaginary parts of a complex mode is treated by Garvey *et al.* [8]. In this paper, complex modes generated by wave propagation through boundaries in infinite structures are investigated. The wave propagation analysis is implemented using a spectral element formulation proposed by Doyle [9]. It is shown that complex modes are somewhere between purely reverberating standing waves (real-mode pattern) and purely propagating waves (wave propagation pattern).

2. MODE COMPLEXITY FACTORS

In this investigation, two different factors for measuring mode complexity are introduced. The first one, used here for complicated structures, consists of the correlation coefficient between the real and complex parts of a certain mode shape vector. This correlation coefficient β_r^2 is computed as

$$\beta_r^2 = \frac{|X_r^{\mathrm{T}} Y_r|^2}{|X_r^{\mathrm{T}} X_r||Y_r^{\mathrm{T}} Y_r|}, \tag{1}$$

where X_r and Y_r are the real and imaginary parts, respectively, of the rth mode shape vector, including all the degrees of freedom of the structure. Note that, for real normal-mode

shapes, β_r^2 must have a unit value. On the other hand, β_r^2 should theoretically be zero for pure wave propagation ODS. The second factor, used for simple unidimensional mode problems, is calculated by curve-fitting the mode to an ellipse in the complex plane, and estimating its radii. Curve-fitting is carried out using a non-linear least-squares algorithm. The complexity factor is then calculated as a measure of the breadth of the ellipse as

$$\gamma_r = 1 - r_a/r_b, \tag{2}$$

where r_a and r_b are the minor and the major radii of the ellipse respectively. Observe that for $\gamma_r = 1$, the ellipse degenerates to a straight line (pure real mode), and for $\gamma_r = 0$ it degenerates to a circle (pure complex mode). It is important to note that this elliptical behavior of modes can only be observed when dealing with single-wave-type propagation problems.

3. THE SPECTRAL ELEMENT METHOD

Doyle [9] presented spectrally formulated finite and semi-infinite elements for Timoshenko beams, known as spectral elements. These elements can be used as a tool to investigate wave propagation in beam-type structures. In contrast to the conventional finite elements, this formulation provides solutions which are exact within the framework of the technical theory used, e.g., Euler–Bernoulli or Timoshenko for beams. It is based on the exact shape functions and the exact mass distribution within each structural element. This analysis provides an accurate dynamic characterization of beam-type structures. In general, a structure is discretized in a small number of spectral elements (one for each span between two discontinuities) and then these elements are assembled in an analogous way to that of the FEM. The main difference is that the calculations in SEM are all carried out in the frequency domain. Time-domain responses can be obtained by performing an inverse FFT. SEM can be seen as a combination of the exact spectral methods and the assembling features of FEM.

Two different types of beam elements can be used in this method: two-noded and throw-off, the latter being a semi-infinite element. The Timoshenko beam spectral element obeys the following equations of motion:

$$\begin{aligned} GA\kappa\left[\frac{\partial^2 v}{\partial x^2} - \frac{\partial \phi}{\partial x}\right] &= \rho A \frac{\partial^2 v}{\partial t^2}, \\ \frac{\partial}{\partial x} EI \frac{\partial \phi}{\partial \mathrm{x}} + GA\kappa\left[\frac{\partial v}{\partial x} - \phi\right] &= \rho I \frac{\partial^2 \phi}{\partial t^2}, \end{aligned} \tag{3}$$

where $GA\kappa$ is the shear stiffness, EI is the bending stiffness, ρA and ρI are the corresponding inertia terms, κ is a geometrical constant that depends on the shape of the cross-section, and v is the transverse displacement. Spectral analysis represents the solutions in the form

$$u(x, t) = \sum \hat{u} \mathrm{e}^{-\mathrm{i}(kx - \omega t)}, \tag{4}$$

where k is the wave number.

For the beam waveguide obeying the Timoshenko beam theory, the equation of motion will have a four-coefficient exact solution given as

$$\begin{aligned} \hat{\phi}(x) &= \mathbf{A}\mathrm{e}^{-\mathrm{i}k_1 x} + \mathbf{B}\mathrm{e}^{-\mathrm{i}k_2 x} + \mathbf{C}\mathrm{e}^{-\mathrm{i}k_1(L-x)} + \mathbf{D}\mathrm{e}^{-\mathrm{i}k_2(L-x)}, \\ \hat{v}(x) &= R_1\mathbf{A}\mathrm{e}^{-\mathrm{i}k_1 x} + R_2\mathbf{B}\mathrm{e}^{-\mathrm{i}k_2 x} - R_1\mathbf{C}\mathrm{e}^{-\mathrm{i}k_1(L-x)} - R_2\mathbf{D}\mathrm{e}^{-\mathrm{i}k_2(L-x)}, \end{aligned} \tag{5}$$

where R_1 and R_2 are defined as the amplitude ratios and k_1, k_2 are the wave numbers defined as

$$k_{1,2}(\omega) = \left[\frac{1}{2}\left\{\left(\frac{1}{c_1}\right)^2 + \left(\frac{1}{c_2}\right)^2\right\}\omega^2 \pm \sqrt{\left(\frac{\omega}{c_2}\right)^2 + \frac{1}{4}\left\{\left(\frac{1}{c_1}\right)^2 - \left(\frac{c_3}{c_2}\right)^2\right\}^2 \omega^4}\right]^{1/2} \quad (6)$$

with the constants $c_1 \equiv \sqrt{GA\kappa/(\rho A)}$, $c_2 \equiv \sqrt{EI/(\rho A)}$, and $c_3 \equiv \sqrt{\rho I/(\rho A)}$.

For throw-off elements, the equations of motion can easily be established from equations (5) by putting $\mathbf{C} = \mathbf{D} = 0$, as waves propagate in only one direction. The solution to these equations can be written in terms of the nodal displacements and a relation between the global shear forces and moments and the global nodal degrees of freedom can be established as

$$[\hat{K}_g]\{\hat{u}_g\} = \{\hat{F}_g\}, \quad (7)$$

where $\hat{K}_g$ is the global dynamic stiffness matrix, which is symmetric and generally has complex elements. The individual elements of this matrix can be found in Doyle [9].

When frame structures are analyzed in three-dimensional space, longitudinal and torsional waves also propagate. To model these kinds of waves, spectral rod and shaft elements must be used. The spectral solution for the rod equation of motion is of the type

$$\hat{u}(x) = \mathbf{A}e^{-ik_L x} + \mathbf{B}e^{-ik_L(L-x)}, \quad (8)$$

with $k_L = \omega\sqrt{\rho/E}$. The throw-off element is again obtained by putting $\mathbf{B} = 0$. The torsional spectral element has the same solution except that k_L is exchanged for $k_T = \omega\sqrt{\rho/G}$.

The fact that only one element is needed between any two discontinuities in SEM plays the role of making the number of elements relatively very small when compared to the finite element method. The solution is exactly independently of the element length within the frequency range where the Timoshenko beam theory is valid. Thus, the response at different nodal degrees of freedom can be recovered with less computational cost even when solving this system of equations at each frequency component.

4. CASE STUDY 1: FINITE AND INFINITE BEAMS

In order to illustrate the behavior of finite and infinite systems, four simple beam structures were modelled using SEM, see Figure 1. All beams have the following properties: Young's modulus $E = 1{\cdot}9 \times 10^{11}$ N/m^2, the Poisson ratio $v = 0{\cdot}3$, mass density $\rho = 7800$ kg/m^3, a rectangular cross-section area $0{\cdot}01915 \times 0{\cdot}0031$ m^2, and an internal loss factor $\eta = 0$. All beams are forced to vibrate by a sinusoidal point force F. The simulated FRFs and ODSs were evaluated with a 0·01 m spatial resolution along a 0·5m span.

To investigate the concept of normal modes and stationary waves, the example in Figure 1(a) is used. In this case, the energy propagating through the beam is trapped between the end boundaries. The waves reach the boundaries and rebound. Bouncing back and forth, these waves form a spatially stationary standing-wave pattern where any point on the wave form does not propagate but rather oscillates around a fixed point in space. When vibrating freely, these patterns are linear combinations of the normal modes.

When forced to vibrate by a sinusoidal point force, the response of the beam, in terms of magnitude and phase relative to the excitation force as a function of the excitation frequency, is the frequency response function (FRF). The spatial pattern of each FRF frequency line is an ODS. When damping is small and modes are well separated in

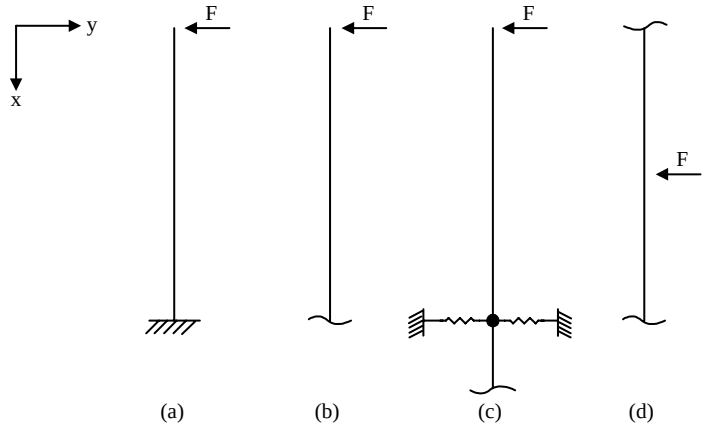

Figure 1. Simple beam structure examples: (a) clamped–free; (b) semi-infinite; (c) semi-infinite with discontinuity, and (d) infinite.

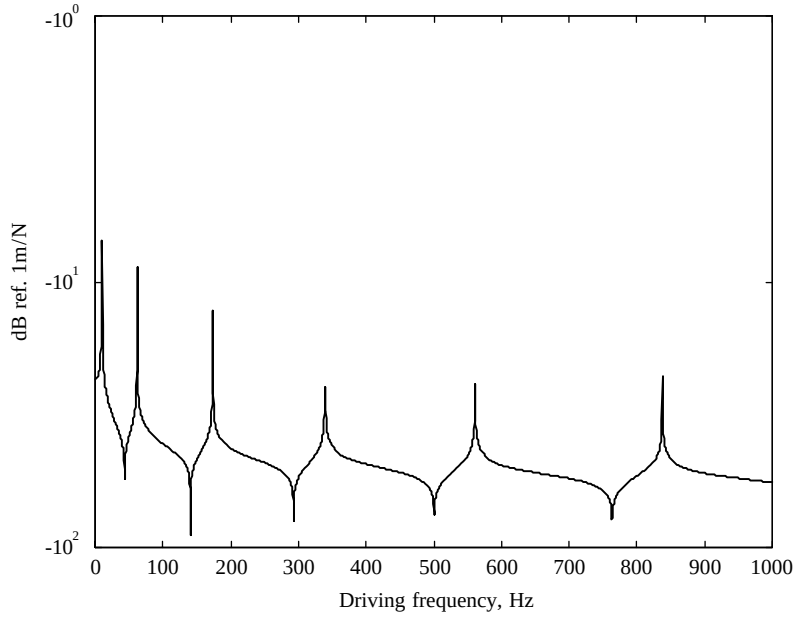

Figure 2. FRF of the clamped–free beam of Figure 1(a).

frequency, the ODS near each natural frequency is very similar to the corresponding mode shape. Figure 2 shows the FRF for the clamped–free beam of Figure 1(a) plotted with a resolution of 0·5 Hz.

In this case, the standing waves pattern for the ODS near the first natural frequency, which is approximately the first normal mode, is plotted in Figure 3.

In order to calculate the mode complexity factor, the modal parameters were identified from the simulated FRFs. The identification was performed using Chebychev orthogonal polynomial method described in reference [10]. The mode shape in this case is real. This can clearly be seen when plotting this mode in the complex plane, Figure 4. The correlation

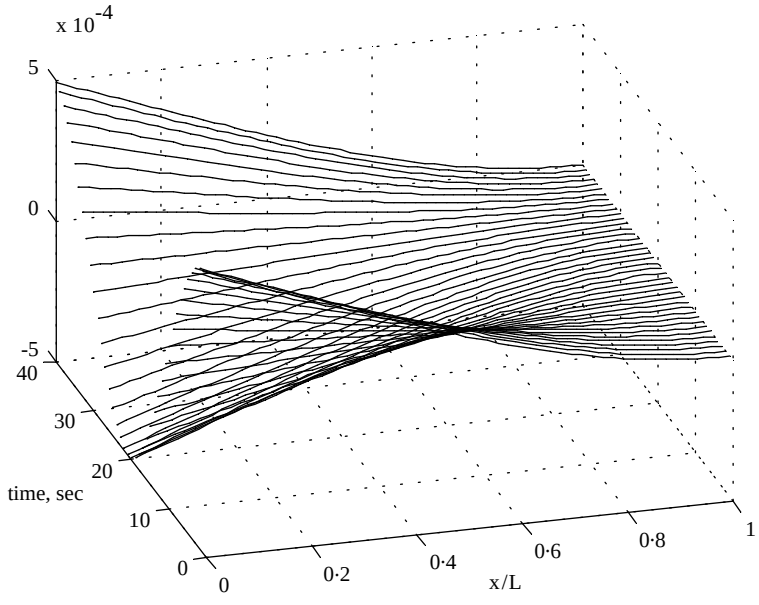

Figure 3. Standing-wave behavior of the ODS of the clamped–free beam at 9·89 Hz.

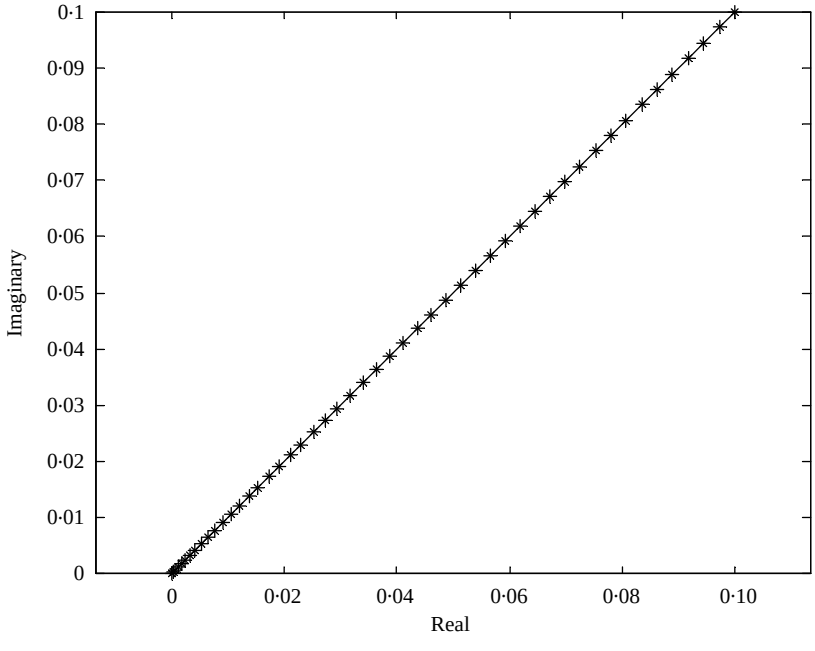

Figure 4. First normal mode of the clamped–free beam in the complex plane.

coefficient β_r^2 (complexity factor) in this case is approximately equal to 1. On the other hand, the other factor γ_r is also equal to 1 as the minor radius $r_a = 0$.

In the second example structure, the semi-infinite beam, instead of standing waves, there is a propagating wave pattern. Energy is no longer trapped within the structure but instead

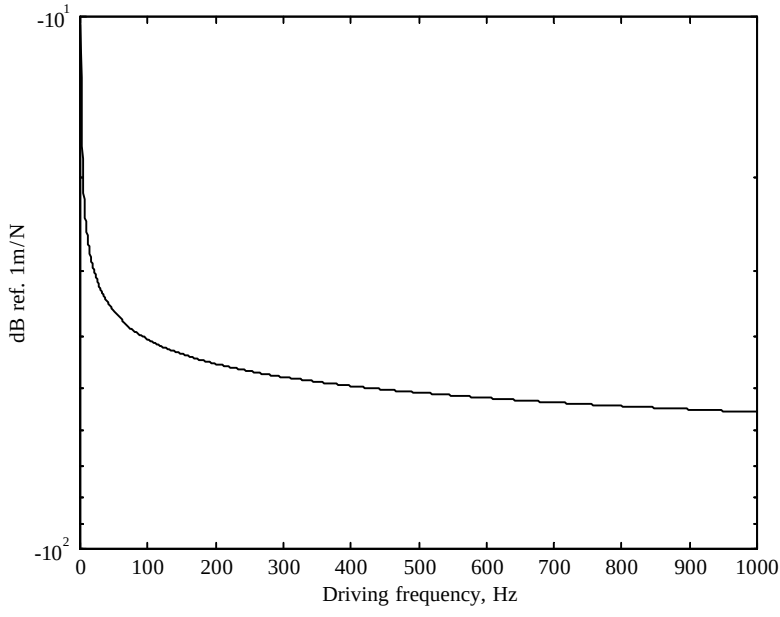

Figure 5. Frequency response of the semi-infinite beam.

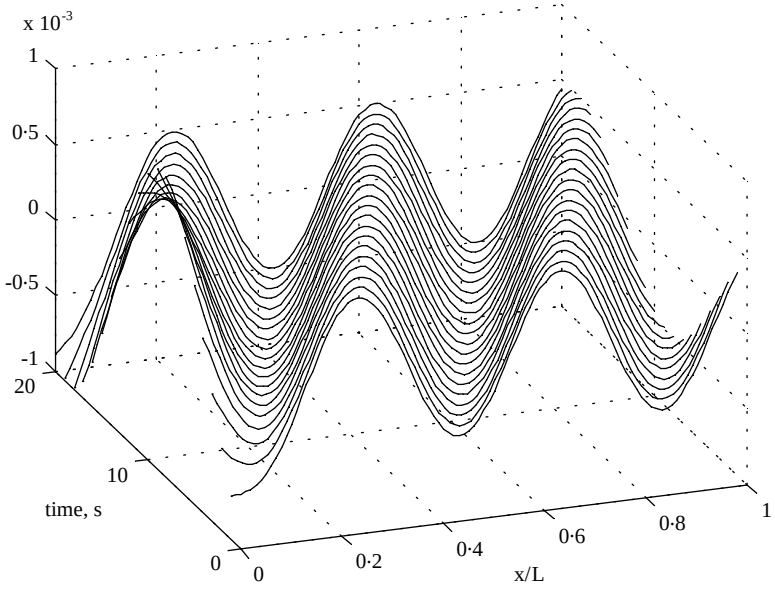

Figure 6. Propagating wave pattern of the semi-infinite beam. ODS at 173 Hz.

it travels towards the infinite end. In this case, no modes are built up and only the ODS can be excited. The frequency response calculated at a point along the beam is shown in Figure 5. Observe that in this case, the FRF does not show any resonance peak and the FRF magnitude decays exponentially with frequency.

In this case, the ODS, can be obtained using the responses computed via SEM at all points in the analyzed frequency. The propagating wave pattern can be observed from the plot in Figure 6.

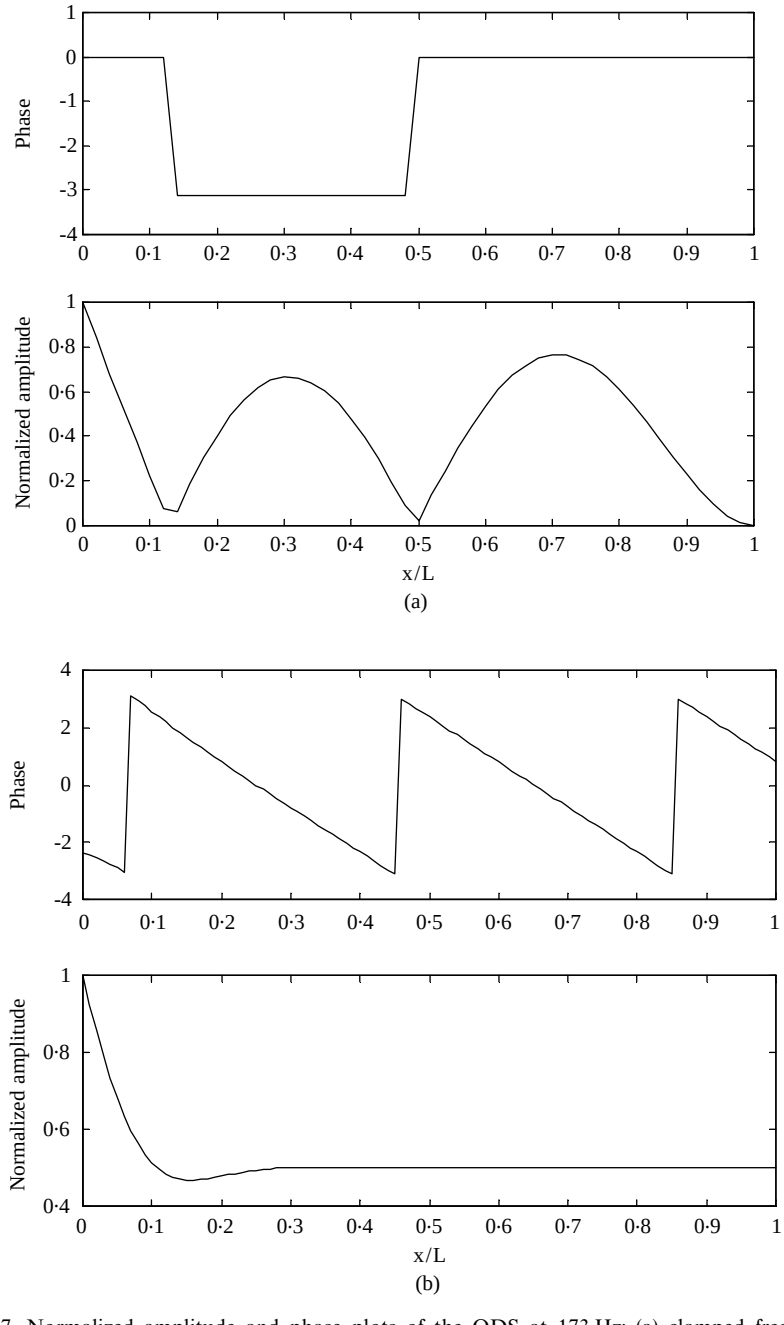

Figure 7. Normalized amplitude and phase plots of the ODS at 173 Hz: (a) clamped–free beam, and (b) semi-infinite beam.

This propagation phenomenon can also be observed in the phase plot of the ODS in Figure 7(b). Note that the phase angles change linearly indicating the axial motion of the flexural waves along the beam. Figure 7(a) shows the corresponding plot for the clamped–free beam for comparison. The operational mode of the semi-infinite beam is complex, as shown in Figure 8, with a complexity factor β^2 of 0·0115. Observe that the plot

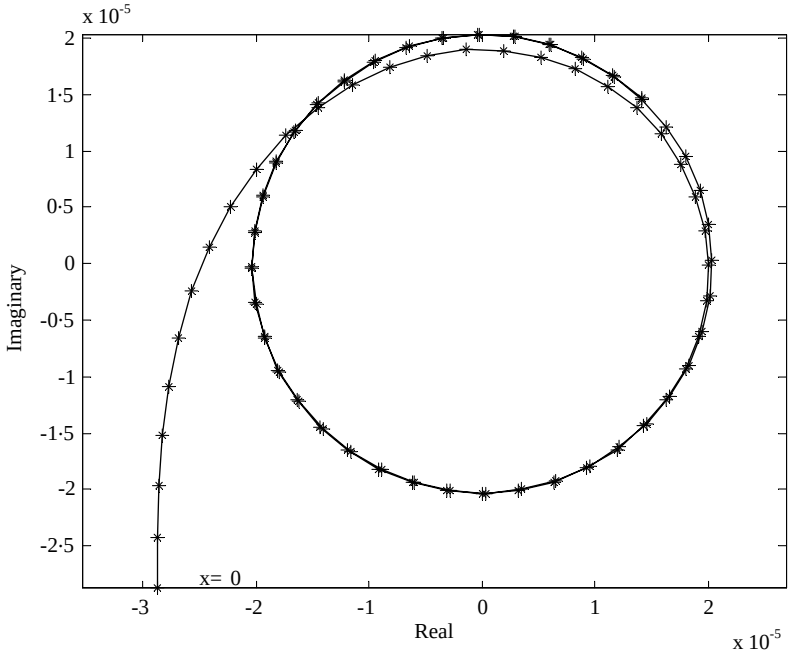

Figure 8. ODS of the semi-infinite beam at 173 Hz in the complex plane.

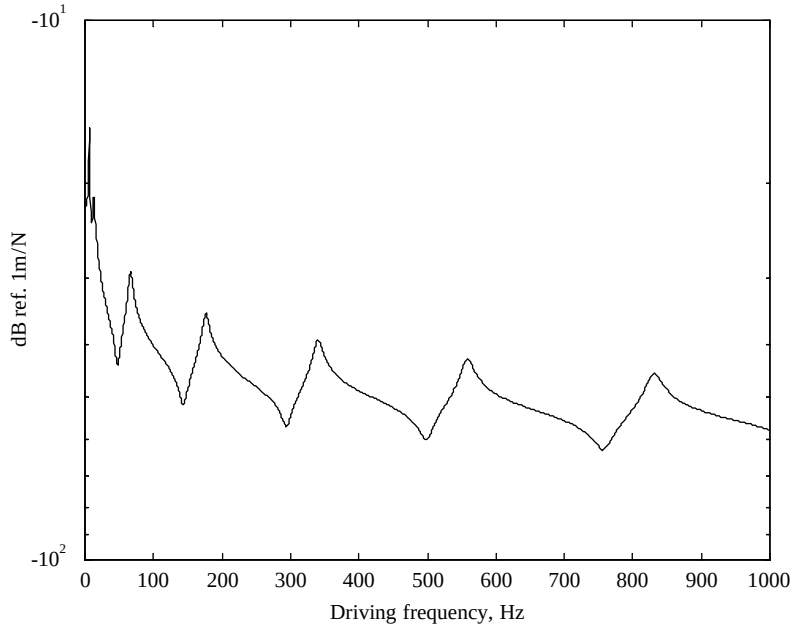

Figure 9. FRF of the semi-infinite beam with discontinuity of Figure 1(c).

of this ODS in the complex plane is not a perfect circle due to the discontinuity represented by the point force at the beam end. The γ_r factor, when calculated at points far from the excitation location, would result in a value of zero, which corresponds to a perfect circle. It should be noted that, in the Nyquist plots, the aspect ratio is set in such a way so that the

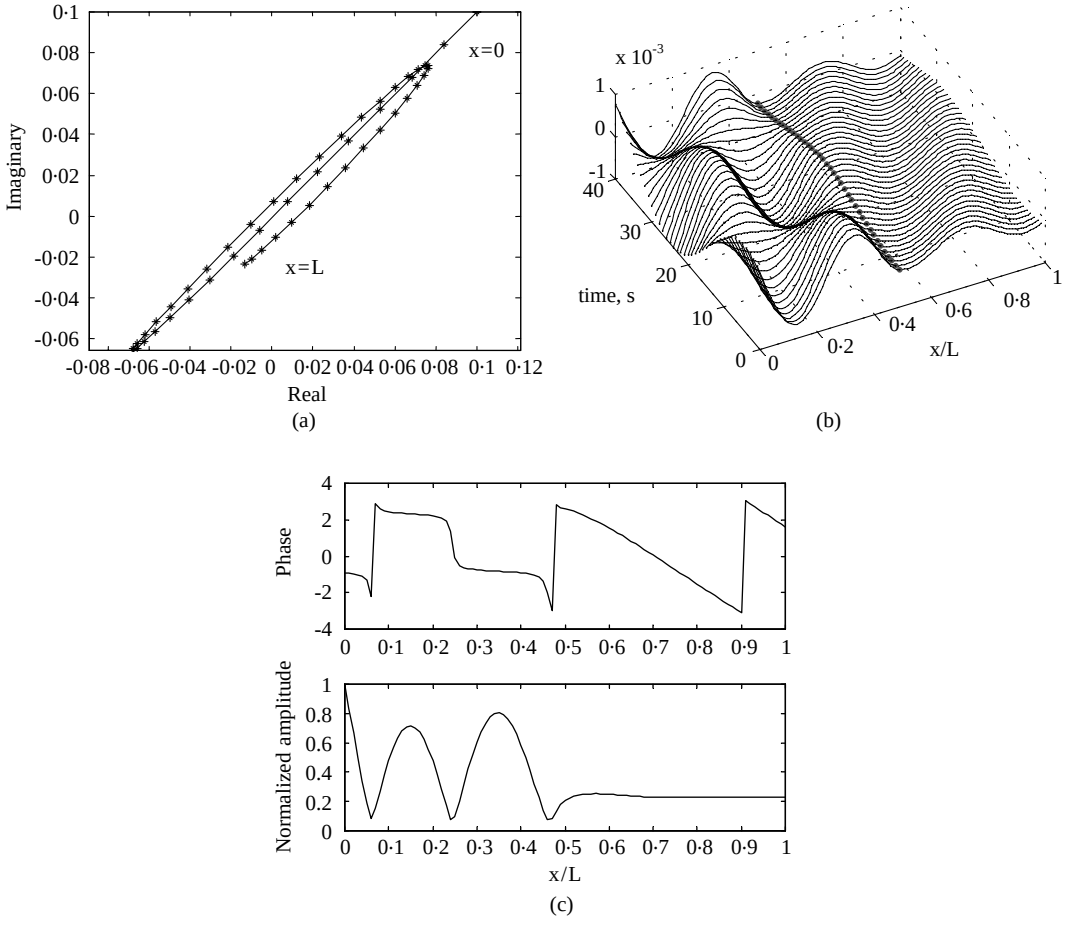

Figure 10. ODS at 176·4 Hz (close to second mode) of the semi-infinite beam with discontinuity: (a) Nyquist plot; (b) vibration pattern; (c) normalized amplitude and phase plots.

tick mark increments, on the x- and y-axis, are equal in size. This makes a circle look exactly like a circle, instead of an ellipse. This is true for all Nyquist plots shown in this paper.

A real structure usually has a combination of the two previously discussed wave types, standing and propagating. One of these cases is when discontinuity is imposed on a straight infinite beam, as the one in Figure 1(c). This discontinuity can be manifested in the form of a massy joint, a localized stiffness element, or two collinearlly coupled beams of different material properties or cross-sections. In the example given here, a lumped mass of 0·1 kg and a linear spring of 1000 N/m stiffness were introduced at a length of 0·5 m from the free end. The infinite length is again represented mathematically by a throw-off spectral element. In this case, the incident flexural waves will travel dispersively along the beam, reach the discontinuity and partly rebound back and partly propagate to infinity. To illustrate the damping effect, the frequency response calculated at the excitation location is shown in Figure 9 (compare with Figure 2).

This structure can be thought of as a beam with one end plunged into a sand box. The second mode shape, of frequency 176·4 Hz, identified using the same modal parameter

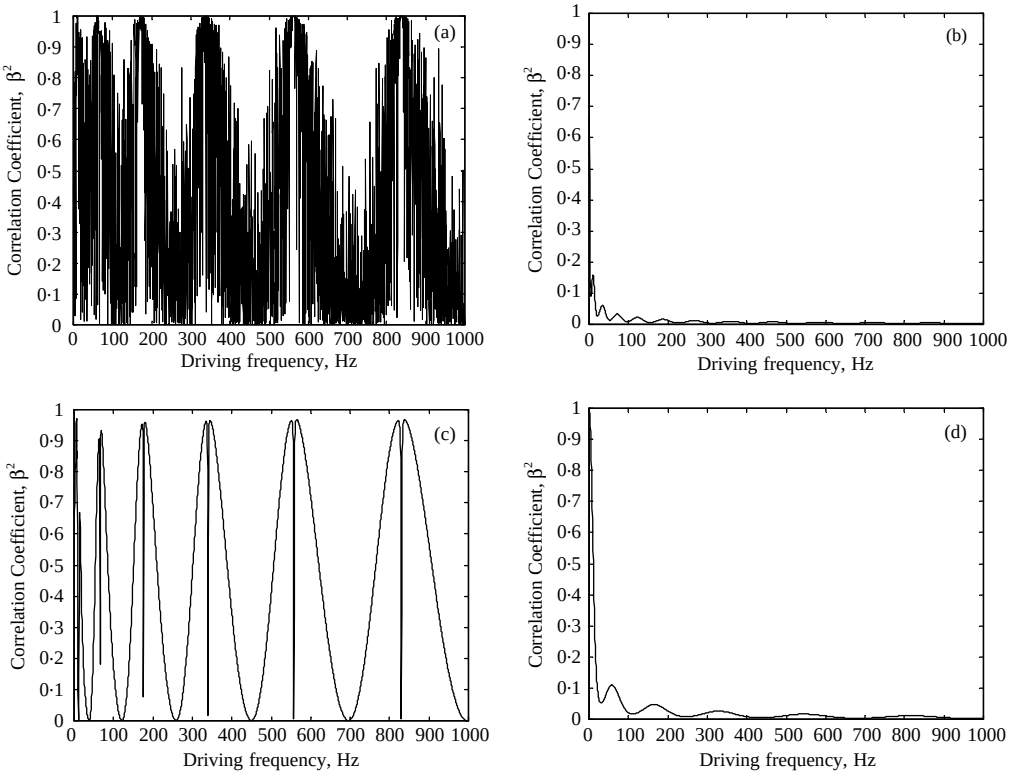

Figure 11. Mode complexity factor as a function of frequency: (a) clamped–free beam, (b) semi-infinite beam, (c) semi-infinite beam with discontinuity (finite part), and (d) infinite beam.

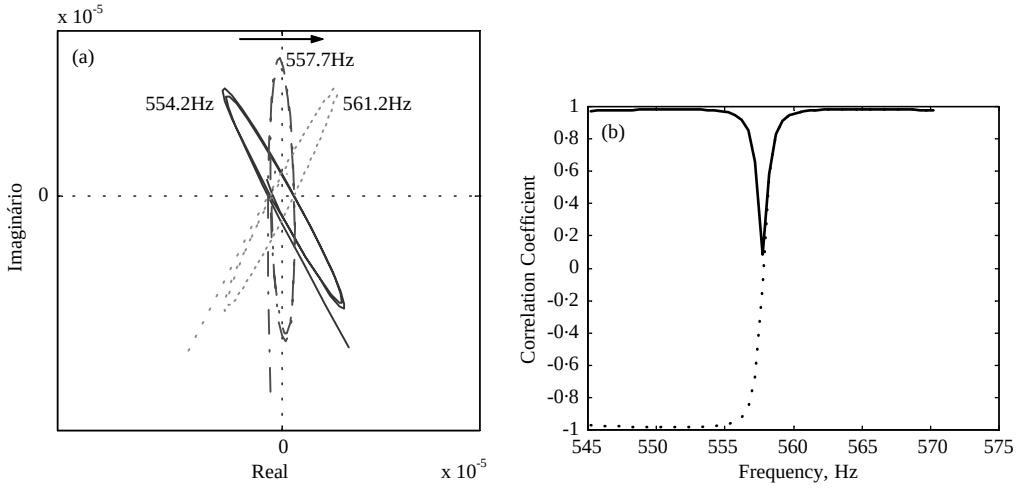

Figure 12. Transition behavior of ODSs from 554 to 561 Hz: (a) complex plane, and (b) complexity factors, shown only for the finite part of the beam structure, ——, β; . . . ., α.

extraction method, is shown in Figure 10(a). The elliptic shape of the mode plotted in the complex plane (only the finite part of the beam displayed) reveals the complex character of the mode.

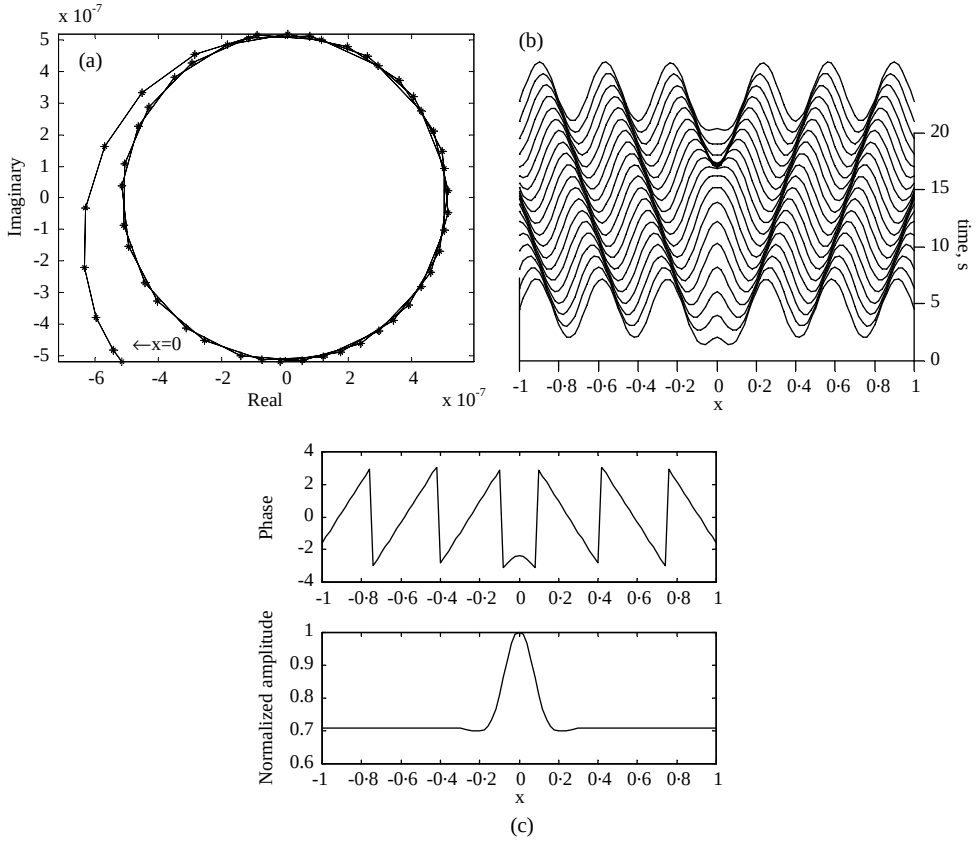

Figure 13. ODS of the infinite beam of Figure 1(d) at 1 kHz: (a) Nyquist plot; (b) vibration pattern, and (c) normalized amplitude and phase plots.

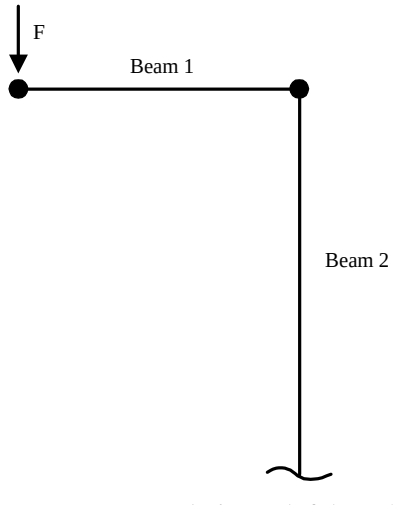

Figure 14. L-shaped beam structure example: *beam* 1 is finite and *beam* 2 is semi-infinite.

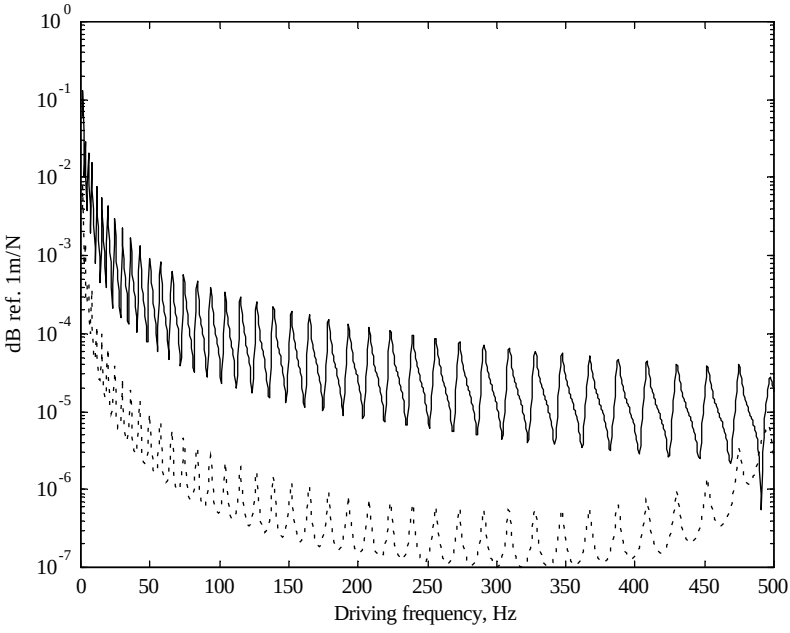

Figure 15. Frequency response of the L-shaped beam. ——, flexural; – – –, longitudinal.

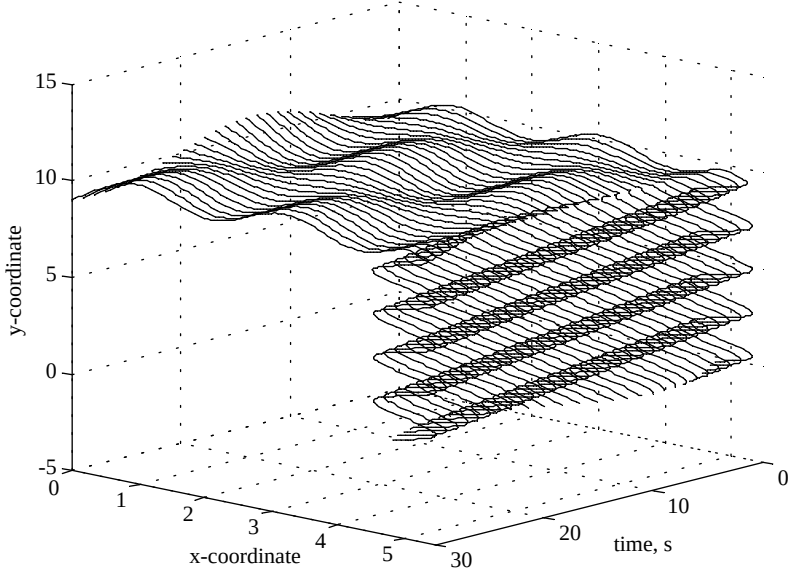

Figure 16. Waterfall plot of the ODS at 5·5 Hz of the L-type beam.

Due to the discontinuity, represented by the massy joint and the localized stiffness elements, the waves in the infinite part propagate with lower, but constant, amplitudes when compared to the ones in the finite part. This can clearly be observed from the waterfall plot of the ODS at 176·4 Hz, Figure 10(b).

Figure 10(c) shows the phase plot of this ODS. The propagating-wave character is clear past the discontinuity, in the infinite section of the beam.

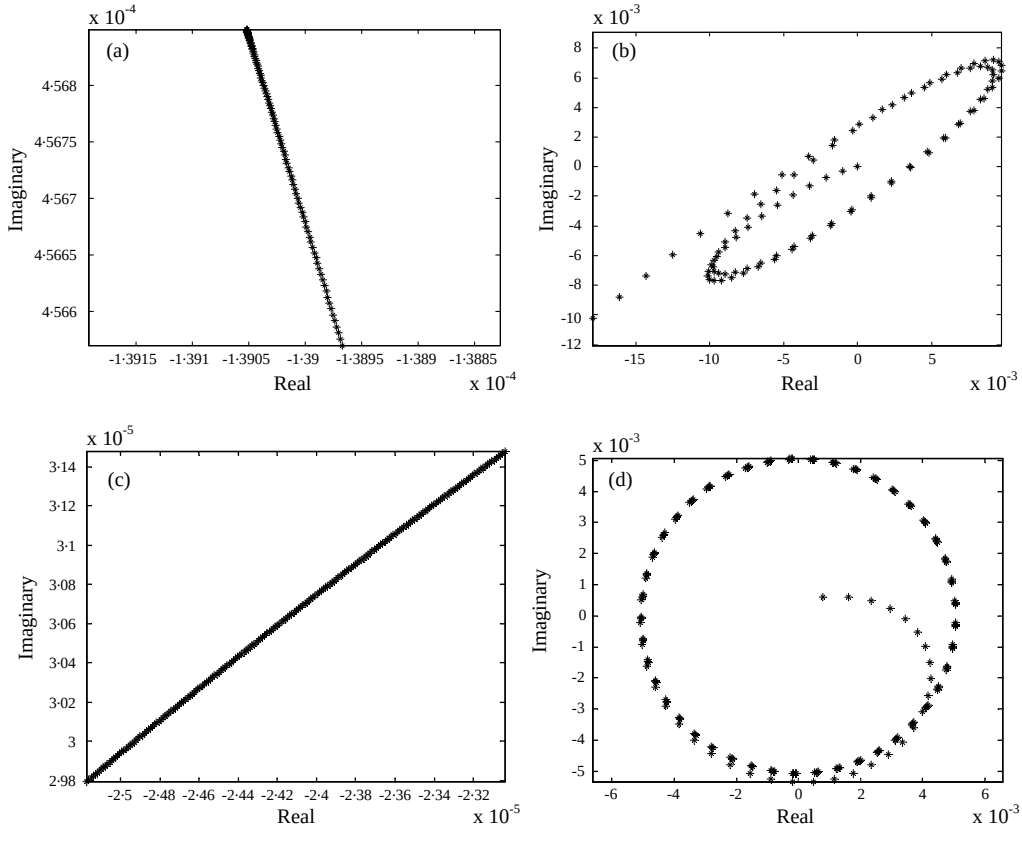

Figure 17. Nyquist plot of ODS at 5·5 Hz: (a) longitudinal waves in *beam* 1; (b) flexural waves in *beam* 1; (c) longitudinal waves in *beam* 2, and (d) flexural waves in *beam* 2.

The mode complexity factor β_r^2 was calculated for the whole frequency range for the three beam structures of Figure 1(a–c). The resulting plots are shown in Figure 11(a–c). For the finite clamped–free beam, β_r^2 has a unity value near the peaks of the FRF, where mode shapes are dominant. On the other hand, the semi-infinite beam only presents values close to zero, as no modes exist but rather, propagating waves.

For the model of the beam with discontinuity (Figure 11(c)), the real or the imaginary part of an ODS passes through the x- or the y-axis at some frequency lines, causing a numerical singularity in the calculation of the β_r^2 factor. This is specifically analyzed in the frequency range where a resonance of, for example, 557·7 Hz lies. The behavior of this resonance in the complex plot, demonstrated only for the finite part of the structure, is shown in Figure 12(a). The correlation coefficient is also calculated through the expression of equation (9), where this coefficient varies from -1 to 1, in contrast to the β_r^2 factor, which is always a positive quantity. Figure 12(b) shows the calculated α_r factor,

$$\alpha_r = \frac{\sum_i (X_i - \bar{X})(Y_i - \bar{Y})}{\sqrt{\sum_i (X_i - \bar{X})^2}\sqrt{\sum_i (Y_i - \bar{Y})^2}}, \tag{9}$$

where $\bar{X}$ and $\bar{Y}$ are the mean values of the X_i's and Y_i's.

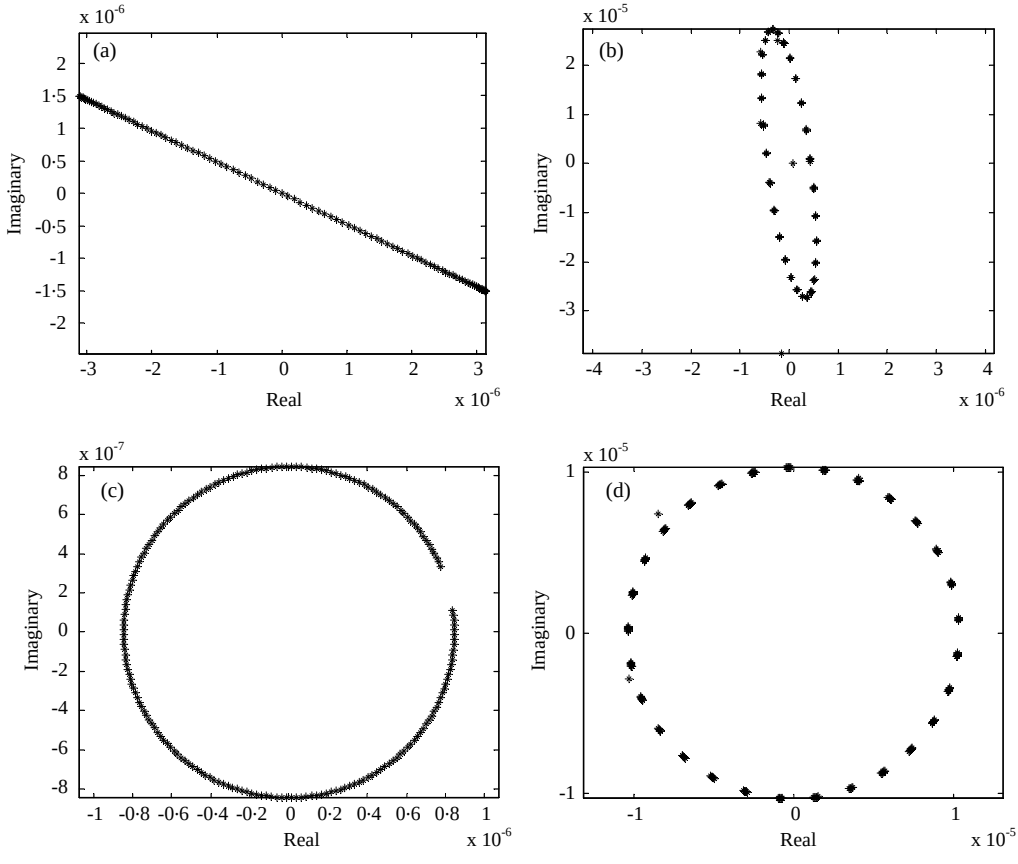

Figure 18. Nyquist plot of ODS at 474·5 Hz: (a) longitudinal waves in *beam* 1, (b) flexural waves in *beam* 1, (c) longitudinal waves in *beam* 2, and (d) flexural waves in *beam* 2.

The notches appearing in Figure 11(c) are due to the crossing of the zero plane causing the singularity in the calculation of the correlation coefficient. In this case, a better option is to estimate the radii of the ellipse and calculate the γ_r factor. At the frequency of 176·4 Hz of the analyzed mode, the γ_r factor is equal to 0·91658.

Finally, an infinite beam excited by a point force shown in Figure 1(d) was investigated. One might think that in this case the complex plot of the ODS would be a perfect circle with zero complexity coefficient. Indeed, this is the result for beam spans far from the excitation location. The point force itself is a discontinuity and, because of it, the circle is distorted in the vicinity of this location. This can be observed in Figure 13(a) which shows the ODS at 1 kHz. Far from the excitation location ($x = 0$), the ODS is a perfect circle. Figure 13(b) shows a waterfall plot of this ODS, where the propagating-wave behavior is clearly observed.

The plot of the complexity coefficient for the infinite beam in the investigated frequency range is shown in Figure 11(d). Figure 13(c) shows the infinite beam ODS phase plot at 1 kHz. The propagating-wave character is clear.

5. CASE STUDY 2: L-SHAPED BEAM

The second case study is an L-type beam which has the same material and cross-section properties used in case study 1. The finite part of the structure, *beam* 1, has a length of

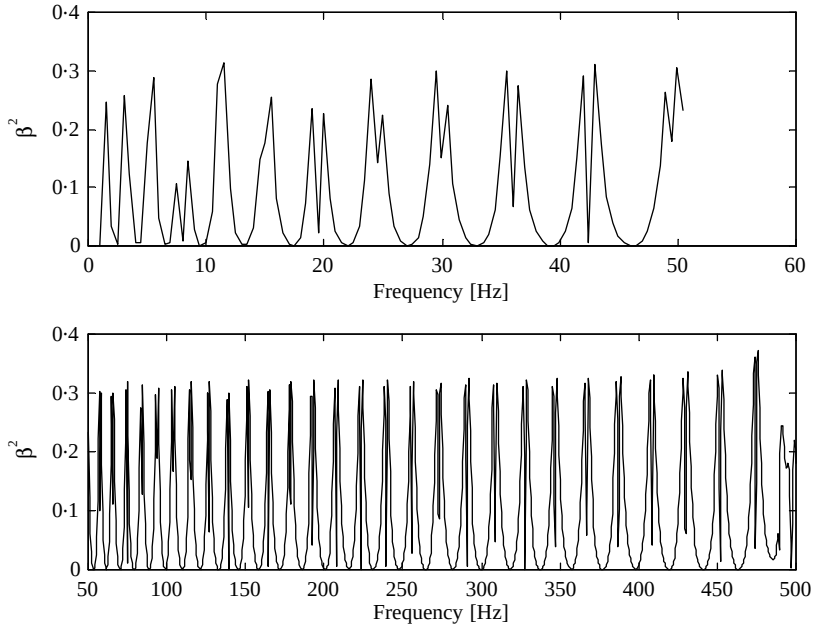

Figure 19. Modal complexity factor for all frequency components.

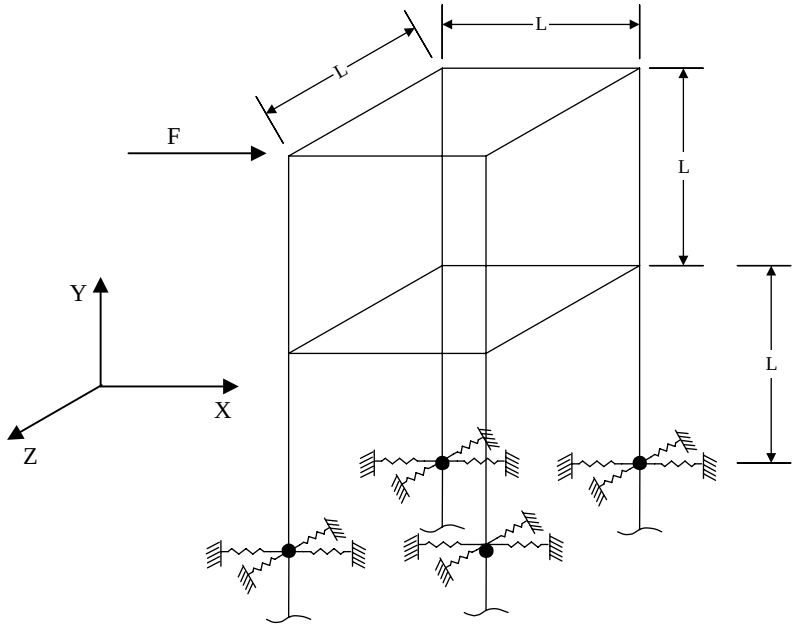

Figure 20. 3-D truss-type structure.

$L = 5$ m, while *beam* 2 is infinite. A length of 10 m is used to show the behavior of *beam* 2. The structure is forced to vibrate by a point force F applied transversally at the free end of *beam* 1 (Figure 14). A frequency range of 1–500 Hz with 0·5 Hz resolution is used. In this case, two kinds of waves are generated: longitudinal and flexural. The numerical simulation

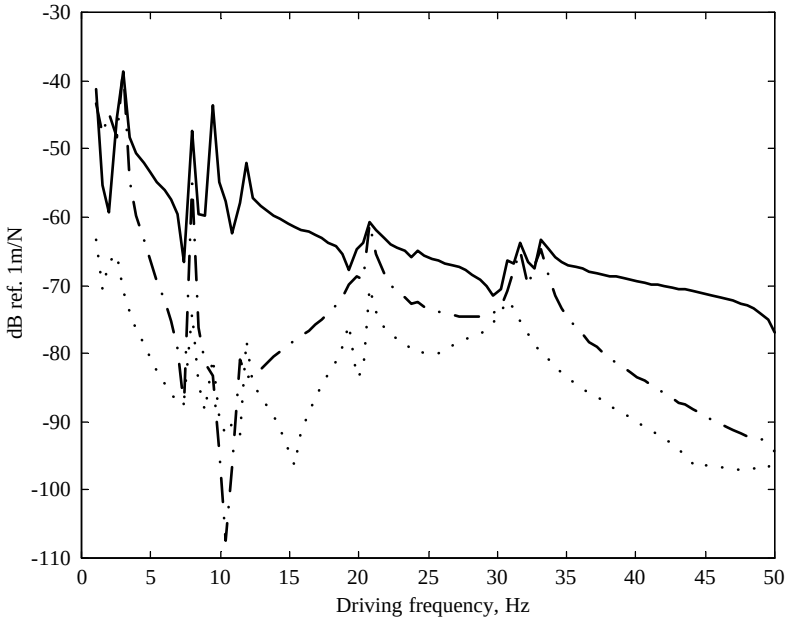

Figure 21. Frequency response at the excitation point, calculated in the three directions: ——, x; – – –, y; - - -, z.

is conducted using the SEM. Only two elements are used: one is two-noded and one is throw-off. The simulated FRFs and ODSs were evaluated with a 0·05 m spatial resolution along both beams. The frequency response calculated at the excitation point is shown in Figure 15.

The ODS near the third resonance (5·5 Hz) is calculated and shown as a waterfall plot in Figure 16. Note the propagation character in *beam* 2 and the stationary-dominated wave character in *beam* 1.

This ODS is characterized by local modes in *beam* 1. The operational mode of the semi-infinite beam is complex as it involves a wave propagation phenomenon. This can be observed from the complex plane plot of this ODS shown in Figure 17(a–d).

It can be noticed that the transverse waves at this frequency are more significant than the longitudinal ones. This can be related to the direction of the excitation force used, which is transverse on *beam* 1. On the other hand, the elliptic shape of the transverse-wave ODS demonstrates the complex character of the ODS. The Nyquist plot of the longitudinal-wave ODS in *beam* 2, shown in Figure 17(c), may be misleading. In fact, what is plotted is a segment of a circle, because the longitudinal wavelength at this frequency is 898·1 m, and only a 10 m span is plotted. The mode complexity factor β^2 of all d.o.f.s for this ODS is 0·28797, which indicates a strong modal complexity. To investigate the mode complexity at higher frequencies, another ODS at a resonance frequency of 474·5 Hz is investigated. In this case, *beam* 2 characterizes a pure wave propagation character. The longitudinal wavelength is 10·4 m and the flexural wavelength is 0·242 m. Therefore, the span of 10 m is sufficient to show the full circle in the Nyquist plot. The mode complexity factor β^2 of all d.o.f.s is 0·03578. The modal complexity of this ODS can clearly be observed from Figure 18(a–d).

From these figures, the stationary longitudinal wave pattern in *beam* 1 is clear. The flexural waves have a purely propagative character in *beam* 2 and a complex modal

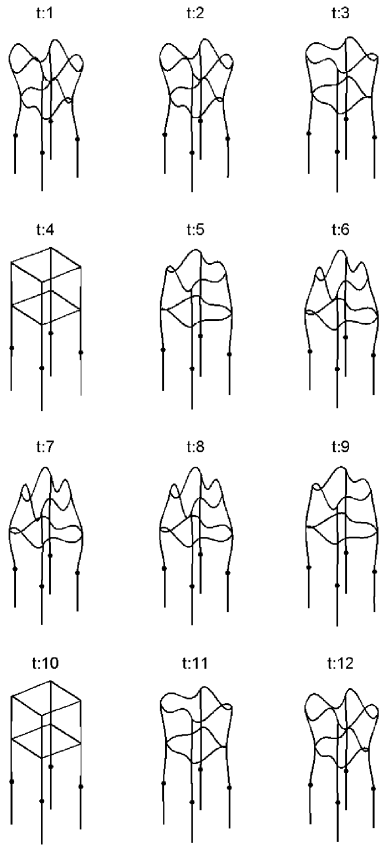

Figure 22. Twelve instant deflections in a vibration cycle of the ODS at 2·98 Hz.

behavior in *beam* 1. On the other hand, longitudinal waves transmitted to *beam* 2 propagate to the infinite end. This is clearly characterized by the perfect circle of the ODS demonstrated in Figure 18(c, d).

The modal complexity factor β_r^2, calculated for all frequency components, is shown in Figure 19. Note that the factor β_r^2 exhibits small values at the resonance frequencies. Again, at resonance the ODS will change phase over a 180° span and at some point it becomes almost purely imaginary causing singularity of the complexity coefficient, as shown back in Figure 12.

Note here that the complexity factor β_r^2 has to be used if the ODS, with all d.o.f.s included, is to be analyzed. The other factor γ_r would only be useful if longitudinal or transverse wave types are to be analyzed separately. The conjunction of all wave types would result in a mixture of lines and ellipses and could not be curve-fitted to one ellipse only.

6. CASE STUDY 3: THREE-DIMENSIONAL FRAME STRUCTURE

A three-dimensional truss-type structure is also investigated. All three kinds of propagating waves in beam, longitudinal, transverse and torsional, are present. The structure is made up of 20 straight steel beams, each with a length of $L = 5$ m. Four of these beams are modelled as throw-off elements, where a mass of 1 kg and localized stiffness elements of 10^6 N/m are added at their nodes. The material and geometry properties are

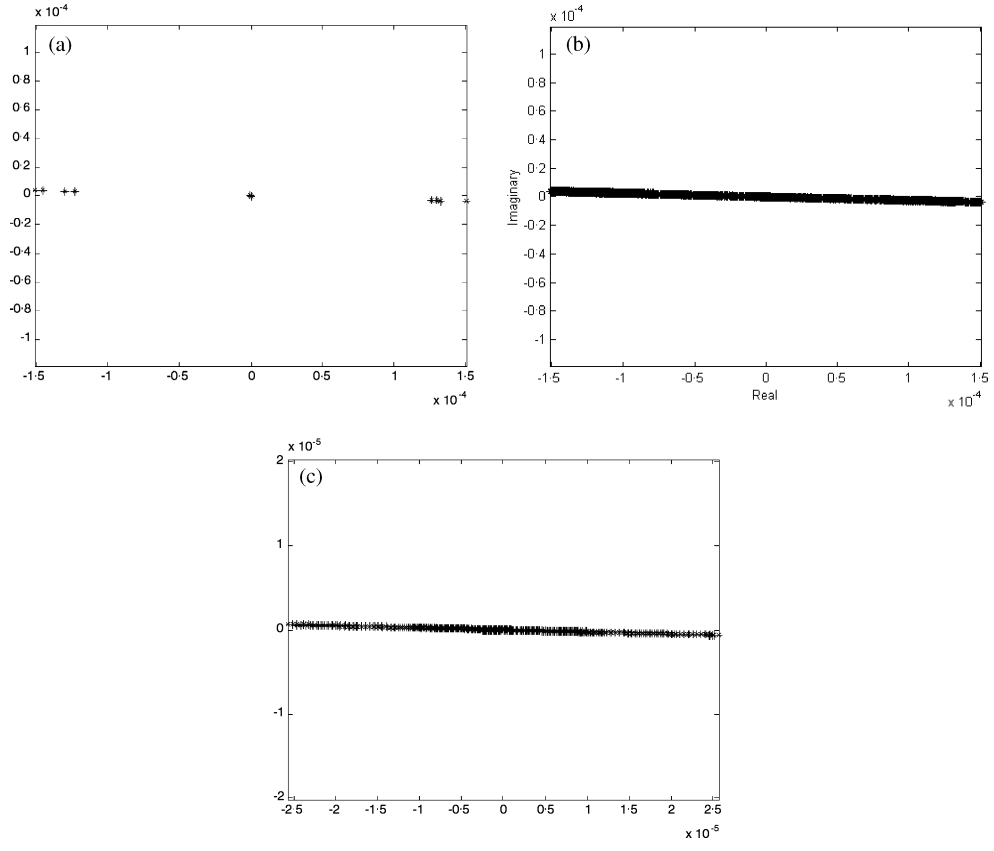

Figure 23. Nyquist plot of the three wave types at 2·98 Hz: (a) longitudinal waves, (b) flexural waves in both planes, and (c) torsional waves.

$E = 2{\cdot}1 \times 10^{11}$ N/m^2, $\rho = 7800$ kg/m^3, $A = 0{\cdot}05 \times 0{\cdot}05$ m^2, $v = 0{\cdot}30$. This type of structure can be thought of as a model to investigate the vibration of real large truss-type structures, which have their bases plunged into the soil. A sinusoidal point force F is applied to the structure as shown in Figure 20.

A frequency range of 1–50 Hz, with a 0·5 Hz resolution is investigated. The frequency response calculated at the three translation d.o.f.s of the excitation point is shown in Figure 21. The ODSs are evaluated with a spatial resolution of 0·05 m.

A low-frequency resonance of 2·98 Hz is first analyzed. This ODS is characterized by deflections defined in the finite members only. Figure 22 shows 12 instant deflections in a vibration cycle of the ODS. The four infinite members have the function of dissipating energy, but exhibit nearly no deflections. This is related to the use of the massy joints and localized stiffness elements, which will decrease the vibrational energy transmitted to the infinite members.

The complexity factor β^2 for this ODS, calculated for the finite members only, is equal to 0·9963, indicating a real-mode character. This ODS is also shown in the complex plane in Figure 23(a–c) for the three wave types in all finite members. The straight line characterizes the real-mode pattern.

At higher frequency, e.g., the ODS near the resonance of 33·17 Hz, the wave propagation phenomenon can be clearly observed in Figure 24. This ODS is complex, with a modal complexity factor β^2 (calculated for the finite members only) of 0·5576.

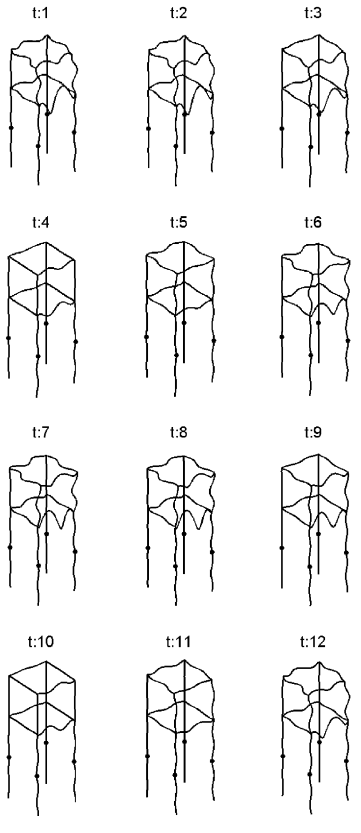

Figure 24. Twelve instant deflections in a vibration cycle of the ODS at 33·17 Hz.

The fact that this mode exhibits a wave propagation pattern can clearly be seen from the complex-plane plot in the three directions (see Figure 25(a–c)).

7. CONCLUDING REMARKS

The main purpose of this work was to present the spectral element method (SEM) as a useful tool in helping to bring back the wave propagation approach to structural dynamic analysis. With the SEM, it is straightforward to model infinite systems and damping caused by wave propagation, which is present in many practical applications. Real structures are not isolated from the neighboring media. Usual boundary conditions such as simple supports and clamps are not realistic in many situations. With the SEM throw-off element, energy dissipation by energy propagation through boundaries can be easily investigated. Also, because the SEM is formulated in the frequency domain, it allows the direct use of experimental impedance measured at the boundaries. How SEM models can be used to investigate and teach modal analysis concepts using exact numerical simulations has been shown (within the context of the adopted beam theory), which would be awkward to do using finite elements.

The aim of the paper is to clarify the ideas about normal and complex modes and show how they can be related to wave propagation phenomena. Modal complexity factors for the quantification of mode complexity have been proposed. Quantification of modal complexity is important in processes of modal testing and model correlation. In general, there seems to be no simple coefficient for the quantification of mode complexity. The

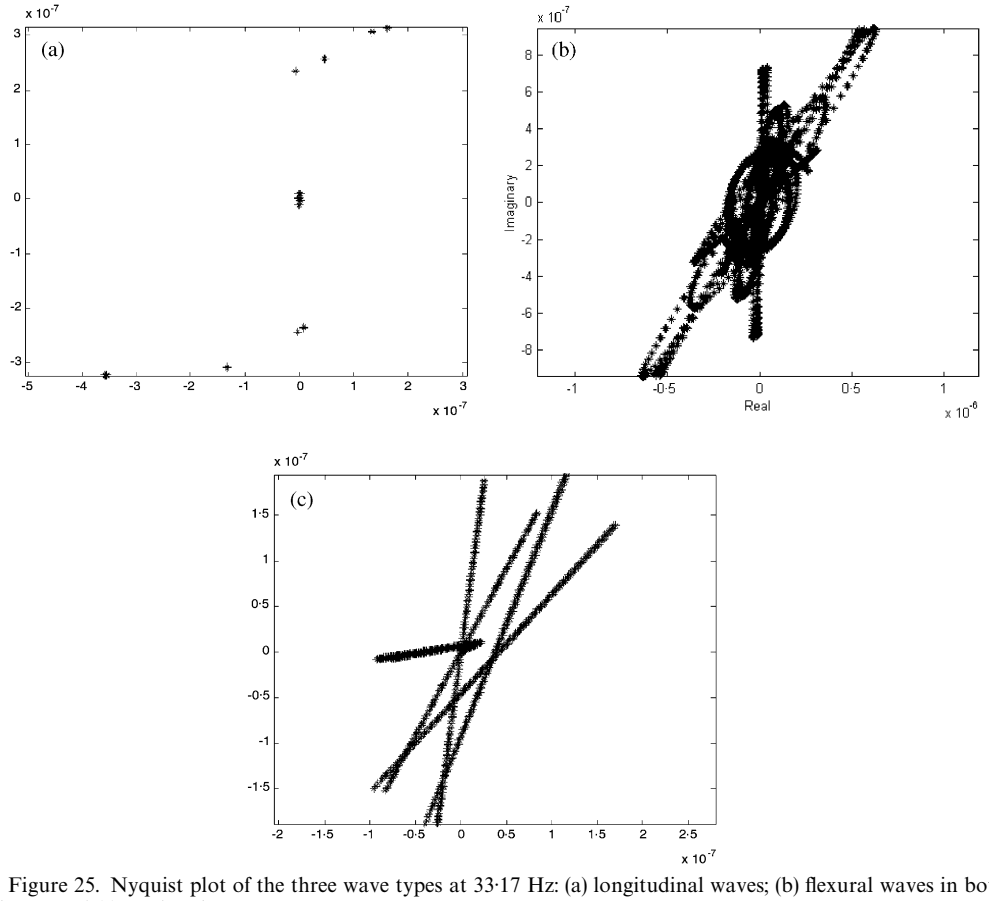

Figure 25. Nyquist plot of the three wave types at 33·17 Hz: (a) longitudinal waves; (b) flexural waves in both planes, and (c) torsional waves.

common procedure is to plot the mode shape or ODS as vectors in the complex plane. The pure real modes are those forming a straight line, and the pure complex modes are those forming a perfect circle. Modes in between have an elliptical shape. Vibration modes of simple structures described by only one type of wave propagation have a well-described distribution when plotted in the complex plane, usually forming an elliptical shape. Mode complexity quantification can be conducted by curve-fitting it to an ellipse, using non-linear least-squares algorithm, and finding the minor and major radii of the ellipse. The breadth of the ellipse could be the measure of mode complexity. Mode complexity of complicated structures, consisting of discontinuities and more wave-type propagation, can be conducted either by analyzing each wave-type alone or through the correlation coefficient between the real and complex parts of the mode. It has been shown that the correlation coefficient is zero in the case of pure wave propagation, far from discontinuities. In the other extreme situation, a finite structure without damping (or with proportional damping) has a complexity coefficient of one.

ACKNOWLEDGMENTS

The authors would like to thank FAPESP (Fundação de Amparo à Pesquisa do Estado de São Paulo) and CNPq (Conselho Nacional de Desenvolvimento Científico e Tecnológico) for the financial support.

REFERENCES

1. D. J. EWINS 1984 *Modal Testing*: *Theory and Practice*. New York: John Wiley.
2. I. IMREGUN and D. J. EWINS 1995 *Proceedings of the* 13*th Intertioonal Modal Analysis Conference*, *Nashville*. Complex modes—origins and limits.
3. S. R. IBRAHIM and A. SESTIERI 1995 *Proceedings of the* 13*th International Modal Analysis Conference*, *Nashville*. Existence and normalization of complex modes in post-experimental use in modal analysis.
4. G. LALLEMENT and D. J. INMAN 1995 *Proceedings of the* 13*th International Modal Analysis Conference*, *Nashville*. A tutorial on complex eigenvalues.
5. L. D. MITCHELL 1990 *Proceedings of the* 8*th International Modal Analysis Conference*, *Kissimmee*, *FL*. Complex modes: a review.
6. G. PRATER Jr 1991 *International Journal for Analytical and Experimental Modal Analysis* **6**, 13–24. Complex modes analysis of non-proportionally damped continuous rods.
7. G. OLIVETO, A. SANTINI and E. TRIPODI 1997 *Journal of Sound and Vibration* **200**, 327–345. Complex modal analysis of a flexural vibrating beam with viscous end conditions.
8. S. D. GARVEY, J. E. T. PENNY and M. I. FRISWELL 1998 *Journal of Sound and Vibration* **212**, 75–83. The relationship between the real and imaginary parts of complex modes.
9. J. F. DOYLE 1997 *Wave Propagation in Structures*: *Spectral Analysis Using Fast Discrete Fourier Transforms*. Berlin: Springer-Verlag; second edition.
10. J. R. F. ARRUDA, S. A. RIO and L. A. SANTOS 1996 *Shock and Vibration* **3**, 127–133. A space-frequency data compression method for spatially dense laser Doppler vibrometer measurements.